September 1976 LRP 117/76

NUMERICAL COMPUTATION OF THE MHD SPECTRUM OF NON-CIRCULAR, SMALL ASPECT RATIO TOKAMAKS

D. Berger, L.C. Bernard, R. Gruber and F. Troyon

This work has been submitted as a contributed paper to the Sixth International Conference on Plasma Physics and Controlled Nuclear Fusion Research, Berchtesgaden (1976).

Centre de Recherches en Physique des Plasmas
ECOLE POLYTECHNIQUE FEDERALE DE LAUSANNE

September 1976 LRP 117/76

NUMERICAL COMPUTATION OF THE MHD SPECTRUM OF NON-CIRCULAR, SMALL ASPECT RATIO TOKAMAKS

D. Berger, L.C. Bernard, R. Gruber and F. Troyon

ABSTRACT

We have developed a spectral code to compute the ideal MHD spectrum of axisymmetric toroidal plasmas of arbitrary cross-section. It is applied to the Soloviev equilibrium. The aspect ratio is kept fixed to 3. The corresponding ratio between the safety factors at the edge and on the axis $q_s/q(0)$ is equal to 1.74. Two different shapes are considered: an almost circular cross-section and a D-shaped elongated cross-section with a half-axis ratio of 2. The two extreme cases of no conducting shell around the plasma and of the shell tight against the plasma surface are treated. The growthrate of the most unstable mode is plotted versus q(0). In the rigid boundary limit we find the low n modes stable above a value of q_0 which is below the Mercier limit. The structure of the modes shows the combined effects of shear and toricity. The calculation is repeated for the free boundary case. The growthrate of the kink plotted versus q(0) has the same general behavior as in the straight case, but the modes show a complicated structure which can be construed as a coupling between an internal mode and a kink of different m through the toricity.

INTRODUCTION

The knowledge of the ideal MHD spectrum is a prerequisite to a good understanding of the behavior of present experiments and to the design of new devices. For large aspect ratio circular cross-section tokamaks, some partial analytical results have been obtained by an expansion in the inverse aspect ratio. For more general configurations, localized criteria have been the only source of information on the existence of an unstable spectrum. This has prompted the development of so-called "spectral codes" in which the MHD spectrum of a configuration is approximated numerically. Such a code which can handle any straight circular cross-section plasma equilibrium has been published [1] and applied to some interesting configurations [2,3]. Generalizations to straight non-circular plasma equilibria have been also described [4,5] and applied to Gajewski's equilibrium [6]. We have recently succeeded in extending our code to uniaxial toroidal configurations [7].

This paper describes a first application of the code to an analytical equilibrium chosen for its simplicity and because it can give plasma shapes similar to JET. We first describe the method and then present the results.

THE NUMERICAL METHOD

The spectrum is obtained by finding the stationary points of the Lagrangian $\mathcal{L} \equiv \delta W_p + \delta W_v - \omega^2 \iiint_p d^3x \rho \underline{\xi}^2$, where δW_p is the usual expression for the plasma potential energy, $\underline{\xi}(\underline{x})$ the displacement, ω the eigenfrequency, ρ the density and δW_v the vacuum potential energy which can be expressed in terms of ξ_n on the surface [8].

In the axisymmetric case, using the non-orthogonal coordinate system (ψ, χ, ϕ) introduced by the Princeton group [4] and Fourier expanding in time and in the ϕ direction $\underline{\xi}(\underline{x}) = \mathrm{Re}\left[\underline{\xi}(\psi,\chi)\, e^{-i m \phi}\right]$, the Lagrangian becomes

$$\mathcal{L} = \tfrac{1}{2} \iint_P \frac{d\sqrt{\psi}}{\sqrt{\psi}}\, d\chi \left\{ \frac{4T^3\psi}{q^3 r^4 B_p^2} \left| F(\chi) \right|^2 + \frac{T^3}{q} \left| \frac{\partial \chi}{\partial \sqrt{\psi}} + \frac{\partial V}{\partial \chi} \right|^2 \right.$$

$$+ \frac{q r^2 B_p^2}{T\psi} \left| \sqrt{\psi} \frac{\partial}{\partial \sqrt{\psi}} \left(\frac{T\chi}{q} \right) + 2\beta \frac{T}{q} F(\chi) - \frac{2\psi_j T}{q r B_p^2} \chi + im\psi T V \right|^2$$

$$+ \frac{\gamma_p T}{q r^2} \left| \frac{\partial}{\partial \sqrt{\psi}} (r^2 \chi) + \frac{\partial}{\partial \chi} (r^2 V) + F(r^2 Y) \right|^2$$

$$\left. - 8 \frac{r^2 T}{q} K \left| \chi \right|^2 \right\}$$

$$+ \oint_S d\chi \oint_{S'} d\chi'\; G(\chi, \chi')\, F(\chi(\chi)) \{ F(\chi(\chi')) \}^*$$

$$- \tfrac{1}{2} \omega^2 \iint_P \frac{d\sqrt{\psi}}{\sqrt{\psi}} d\chi \rho \left\{ \frac{2T\psi}{B_p^2 q} \chi^2 + \frac{q r^4 T}{2} Y^2 + \frac{B_p^2 r^6 q}{2T\psi} \left| \sqrt{\psi} Y + \sqrt{\psi} V - 4\beta \chi \right|^2 \right\}$$

where

$$\chi = q r B_p \xi_\psi / T\,, \quad V = \frac{2\beta\chi}{\sqrt{\psi}} - Y + \frac{2\sqrt{\psi}\,\xi_\chi}{r^2 B_p}\,, \quad Y = \frac{2\sqrt{\psi}\,\xi_\phi}{r T}\,, \quad F = \frac{\partial}{\partial \chi} - imq(\psi).$$

$B_p(\psi, \chi)$ and $T(\psi)/r$ are the poloidal and toroidal components of the magnetic field, j the toroidal current density, $q(\psi)$ the safety factor and $r(\psi, \chi)$ the distance to the main axis of the torus. $G(\chi, \chi')$ is a surface Green's function which depends only on the geometry of the vacuum region.

The code uses a "finite hybrid element" expansion of X, Y and V [7]. The domain $0 \leq \sqrt{\psi} \leq \sqrt{\psi_s}$, $0 \leq \chi \leq 2\pi$, where ψ_s is the value of ψ at the surface, is covered with a rectangular mesh. X is defined at the mesh points and Y and V at points shifted by half a cell in the χ direction. The Green's function is obtained by solving numerically a Fredholm integral equation on the plasma surface and on the conducting shell, using a finite element

expansion [9]. The variational problem reduces then to a matrix eigenvalue equation of the form $A - \omega^2 B = 0$, where B is a positive matrix, which is solved by a fast inverse vector iteration scheme.

In the case where the equilibrium is symmetric with respect to the plane z=0, the domain can be restricted to $0 \leq \chi \leq \pi$.

The results presented in this paper have been obtained with $N_\psi \leq 24$ equal intervals in the ψ direction and $N_\chi \leq 24$ equal intervals in half the range in χ . Convergence has been tested for all the results presented here.

The Equilibrium

Since little is known on the spectrum of toroidal plasmas, we choose for our first try, Soloviev's equilibrium given by

$$\psi(r,z) = \frac{E}{2 q_0} \frac{a^2}{R\sqrt{R^2+b^2}} \left[\frac{r^2+b^2}{E^2} z^2 + \frac{(r^2-R^2)^2}{4} \right]$$

and characterized by four parameters: the aspect ratio R/a, the vertical elongation E, the safety factor on the axis q(0) and b. It has the advantage of being analytical, simple, and of reducing in the limit of a large aspect ratio to Gajewski's equilibrium, the spectrum of which is known. Also with the four parameters it is possible to produce a variety of shapes with substantial shear.

In this paper we restrict ourselves to the cases b = 0 ($\beta_p = 1$), R/a = 3, with either an infinite vacuum region surrounding the plasma or with no vacuum region at all (rigid boundary). Note, that there is already a substantial amount of shear since with these parameters $q(\psi_s)/q(0) = 1.74$. We also assume constant density ρ .

RESULTS

There are still two free parameters to characterize the equilibrium, q(0) and E. We follow the usual way of representing the growthrates versus q(0) for fixed E. To make the comparison with other authors [4,6] easier, the growthrate $\Gamma = i\omega$ is normalized with the poloidal Alfvèn frequency $\omega_A = \frac{T}{\sqrt{\rho}\, q(0) R^2}$. We consider successively four cases: E = 1 and E = 2 with and without vacuum. The case E = 1 is interesting because it reduces to the circular case when R/a >> 1. E = 2 gives an elongated D-shape cross-section very close to the JET design.

Internal Rigid Boundary Modes

We first consider the case with the conducting shell tight against the plasma, which is equivalent to dropping the vacuum potential energy term and imposing the boundary condition $X(\psi_s, \chi) = 0$.

a) E = 1

The square of the growthrates of the most unstable modes are shown in Fig. 1 as functions of q(0) for n = 2,3 and 4. For n = 1 we did not find any unstable modes. More precisely, we found unstable modes with decreasing growthrates as the number of elements increased, and the extrapolation to an infinite number of elements led to stable or close to marginal modes. There could still be some surprises here, but if there are unstable modes their maximum growthrate will be at least one order of magnitude smaller than the maximum growthrate of the n = 2 modes. This point illustrates an essential difference between the discretization scheme used here and the standard finite element method. In the latter, the discretization error is stabilizing while it is destabilizing with our method. To discuss the results, it is useful to introduce an azimuthal number $m(\psi) \equiv \left| \text{Arg } X(\psi, 2\pi) - \text{Arg } X(\psi, 0) \right| / 2$. It is an integer which reduces to the usual azimuthal number m in straight circular geometry. On each figure the range of q(0) in which the singular surface $nq(\psi) = \ell$ (integer) lies inside the plasma is shown by a

segment identified by ℓ . For example, for n = 2 the surface nq = 1 lies inside the plasma when $.287 < q(0) < .5$. For n = 2 there are two unstable regions. The mode which peaks at q(0) = .4 is a pure m = 1 mode near its maximum becoming mixed with m = 2 or m = 0 in the wings. The unstable modes at low q values is mostly m = 0, with almost no deformation of the magnetic surfaces. The same resonant structure is visible in the n = 3 and 4 curves, but the modulation attenuates as n increases. The first peak starting from the left is pure m = 1, the second is mostly m = 2 with m = 3 near the surface. The third peak in n = 4 is mostly m = 3 with m = 4 near the surface. As n increases, more resonant surfaces can lie simultaneously in the plasma, leading to complicated m profiles. This seems to have a stabilizing influence. A comparison between the three cases brings some interesting points. All the modes have a toroidal component of the same order of magnitude as the other two components. The stability limit remains below the Mercier limit q(0) = 1. The limit increases with n probably accumulating at q(0) = 1 as $n \longrightarrow \infty$. Under the Mercier limit there is room for one more unstable resonant region with $m \approx n$, but it is not there. Analogous results have been obtained by Wesson [10] and Kerner [11]. For each n we have plotted only the most unstable mode. There are other modes with smaller growthrates. We did not search systematically for them.

b) E = 2

Figure 2 shows the results for n = 1,2 and 3. They are very analogous to the E = 1 case. Let us concentrate rather on the differences. All the modes are strongly destabilized. There is now an unstable n = 1 mode. Near the peak at q(0)= .8 this mode is pure m = 1. Plugging back the eigenvector into δW_p, we see that the negative contribution comes from the region with strong unfavorable curvature. Summing over each magnetic surface we see that only an inner region gives a negative contribution. This region is not limited by q = 1 as in the straight geometry; for example, when q(0) = .8 the last surface unstable is at q = .83. The mode though is not confined to the region $q < 1$ as $|X|$ decreases regularly from the center to the surface. Note, that the growthrate of this mode remains small. For n = 2 the first peak on the left is still a pure m = 1 mode. Here too, it is the inner magnetic surface

which is unstable and the marginal surface corresponds to a value nq substantially below 1. The second peak corresponds to a mode which is mainly m = 2 with m = 1 near the center and m = 3 close to the surface. The n = 3 modes have the same behavior. The presence of the peak with m = n dominant in the three cases pushes the stability limit to $q(0) \approx 1.1$, which is still substantially below the Mercier limit $q(0) = 1.35$. There is no evidence yet that the limit will move up to the Mercier limit as n increases, contrary to the case E = 1. The same drop in growthrate as the number of singular surfaces in the plasma increases is observed. One should also make the same remark as for n = 1, E = 1, concerning the difficulty of ascertaining that there are no unstable modes in a given region. We cannot exclude the possibility of very weakly growing modes in the region between q(0) = 1.1 and the Mercier limit.

These rigid boundary results are rather surprising. It implies that if q(0) is lowered adiabatically it is the high n, high m Mercier modes which become first unstable, contrary to the case of a straight column.

Free Boundary Modes

We consider now the case where the plasma is surrounded by an infinite vacuum region. This is the domain of the external kinks. In the limit of a large aspect ratio the growthrate of the kink is only a function of nq(0). This means that only one value of n needs to be examined. With an aspect ratio of 3 we expect to see corrections to this result.

a) E = 1

The square of the growthrates of the most unstable mode for n = 1 and n = 2, plotted versus q(0), are shown in Fig. 3. The curves have a periodic structure, the period being given by $\Delta q(0) \approx 1.74/n$. The minima coincide with the presence of a singular surface near the plasma surface, just as in a straight system. The differences with a nq dependence are visible, specially for the first peak which is more important for n = 2 than for n = 1. The

modes all have a very small component of the displacement in the toroidal direction, contrary to the internal modes where the three components are comparable. Looking at the structure of the modes there is little difference between the n = 1 and n = 2 modes so that we shall discuss them together. Starting from the left, the first peak is a pure m = 1 mode with an essentially rigid motion. All the magnetic surfaces are unstable. The second peak is m = 2 at the surface and m = 1 inside. Figure 4 shows the motion in a meridian plane, chosen such that the mode be symmetric, for q(0) = .45 and n = 2. The motion in the center is m = 1 and connects to the m = 2 motion at the surface. The length of the arrows indicate the relative magnitude of the displacement. The axis of the torus is on the left, the motion being towards the outside. The motion is mostly m = 1 and yet the main destabilizing contribution comes from the region where m = 2. We visualize this mode as a coupling through toricity of an unstable m = 2 kink with an almost marginal internal m = 1 mode. This interpretation is supported by the fact that there is a q = 1 singular surface in the plasma. Similarly the next peak will be m = 3 near the surface and m = 2 inside, and so on. Looking at the 5th peak, which is the last one we have computed and the first to have two singular surfaces in the plasma, we see that it is made of a central m = 3 region with almost no motion, m = 4 intermediate region and m = 5 narrow layer near the surface. There again, most of the destabilizing contribution comes from the vicinity of the surface.

b) E = 2

Figure 5 shows the results for n = 1. Compared to E = 1 the curve has the same periodic behavior with only slight shifts in the maxima and minima. There is a strong destabilization of the m = 1 mode and a stabilizing trend in the high q(0) region which we could not follow because of computing limitations. The structure of the modes remains very similar to E = 1.

c) Internal modes

We have not yet searched systematically for the other unstable "internal modes" which lie below the kink with growthrates comparable to those of the rigid boundary modes. We do have some partial results which show that there

exist unstable modes made up of an internal part coupled to an external kink mode. An example of such a mode is shown in Fig. 6 for the same parameters as in Fig. 5, namely E = 1, n = 2, q(0) = .45. The mode has an internal m = 1 part which looks like an internal kink with an external m = 2 kink-like behavior in the outside region. Its growthrate $\Gamma^2/\omega_a^2 \approx .025$ is typical of internal modes. The map of the potential energy shows an unstable core and an unstable region at the surface separated by a large essentially neutral layer.

ACKNOWLEDGMENTS

We thank the staff of the Computing Center for their help. Throughout the development of our code and now during the exploitation we have maintained a constant interaction with the Princeton group which is also developing such a code.

This work is supported in part by the Swiss National Science Foundation.

REFERENCES

[1] APPERT, K., BERGER, D., GRUBER, R., TROYON, F., ROBERTS, K.V. Computer Phys.Commun. 10 (1975), 11

[2] BOREL, D., APPERT, K., BERGER, D., GRUBER, R., TROYON, F., ZAMP 26 (1975), 656

[3] POCHELON, A., KELLER, R., TROYON, F., GRUBER, R., 7th European Conf. on Contr.Fusion and Plasma Phys. Vol. I (1975), 157

[4] CHANCE, M.S. et al. in "Plasma Physics and Controlled Nuclear Fusion Research (1974)". (International Atomic Energy Agency, Vienna, 1974), Vol. 1, p. 463

[5] GRUBER, R., APPERT, K., BERGER, D., DEBONNEVILLE, F., TROYON, F., 7th European Conf.on Contr.Fusion and Plasma Phys. Vol. I (1975), 108.

[6] CHANCE, M.S., GREENE, J.M., GRIMM, R.C., JOHNSON, J.L., MATT-1246 (May 1976), Princeton University

[7] BERGER, D., GRUBER, R., TROYON, F., 2nd European Conference on Computational Physics (1976). C3

[8] LUST, R., MARTENSEN, E., Z.Naturforschung 15a (1960) 706

[9] BERGER, D., BERNARD, L.C., GRUBER, R., TROYON, F., ZAMP, to be published

[10] SYKES, A., WESSON, J.A., IAEA-CN-33/A12-3, Tokyo (1974)

[11] KERNER, W., MATT-1229 (March 1976), Princeton University

FIGURE CAPTIONS

Figure 1: The square of the normalized growthrate Γ^2/ω_a^2 of the most unstable modes versus the safety factor on the magnetic axis q_0. Rigid boundary case. E = 1 and n = 2, 3 and 4.

Figure 2: The square of the normalized growthrate Γ^2/ω_a^2 of the most unstable modes versus q_0. Rigid boundary case. E = 2 and n = 1, 2 and 3.

Figure 3: The square of the normalized growthrate Γ^2/ω_a^2 of kink modes versus q_0 for n = 1 and 2. Infinite vacuum region surrounds the plasma (no shell). E = 1.

Figure 4: Map showing the instantaneous displacement in a meridian plane chosen such that the flow be symmetrical about the mid-plane. The mode represented is a kink with E = 1, q_0 = .45 and n = 2. Note, that m = 1 in the center and m = 2 on the outside.

Figure 5: Plot of the normalized growthrate Γ^2/ω_a^2 of the E = 2, n = 1 kink mode versus q_0.

Figure 6: The instantaneous displacement in a meridian plane of the second most unstable mode for E = 1, q_0 = .45 and n = 2 (same parameters as in Fig. 4). The vertex in the central region distinguishes it from the kink mode. The growthrate Γ^2 is about twenty times smaller than for the kink.

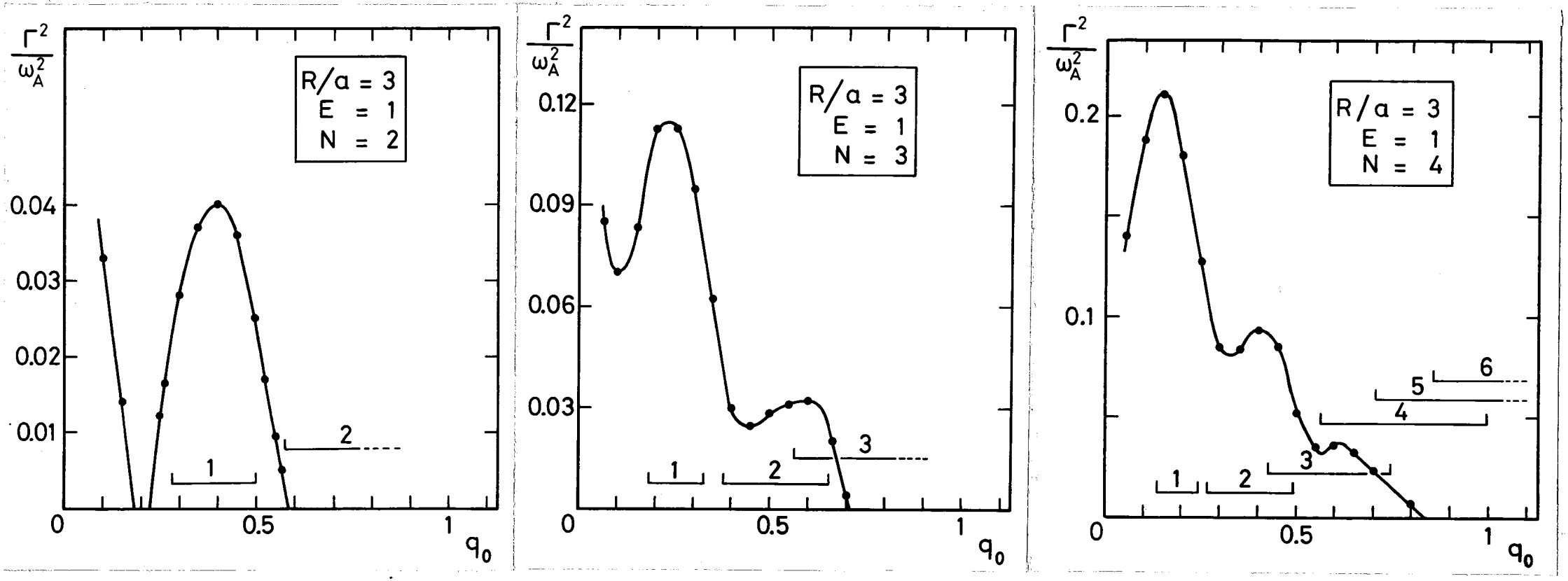
$\frac{\Gamma^2}{\omega_A^2}$
R/a = 3
E = 1
N = 2
0.04
0.03
0.02
0.01
0
0.5
1
q_0
1
2
$\frac{\Gamma^2}{\omega_A^2}$
R/a = 3
E = 1
N = 3
0.12
0.09
0.06
0.03
0
0.5
1
q_0
1
2
3
$\frac{\Gamma^2}{\omega_A^2}$
R/a = 3
E = 1
N = 4
0.2
0.1
0
0.5
1
q_0
1
2
3
4
5
6

FIGURE 1

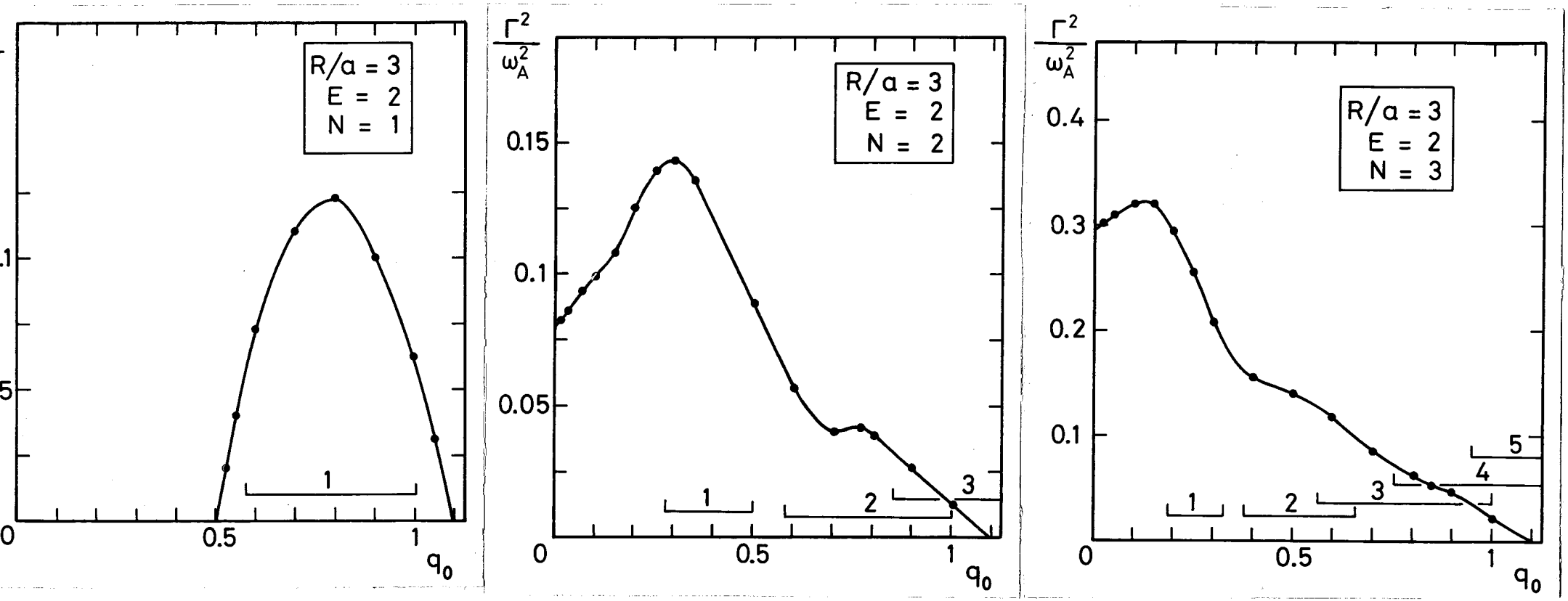
R/a = 3
E = 2
N = 1
1
0.5
1
q_0
$\frac{\Gamma^2}{\omega_A^2}$
0.15
0.1
0.05
0
R/a = 3
E = 2
N = 2
1
2
3
0.5
1
q_0
$\frac{\Gamma^2}{\omega_A^2}$
0.4
0.3
0.2
0.1
0
R/a = 3
E = 2
N = 3
1
2
3
4
5
0.5
1
q_0

FIGURE 2

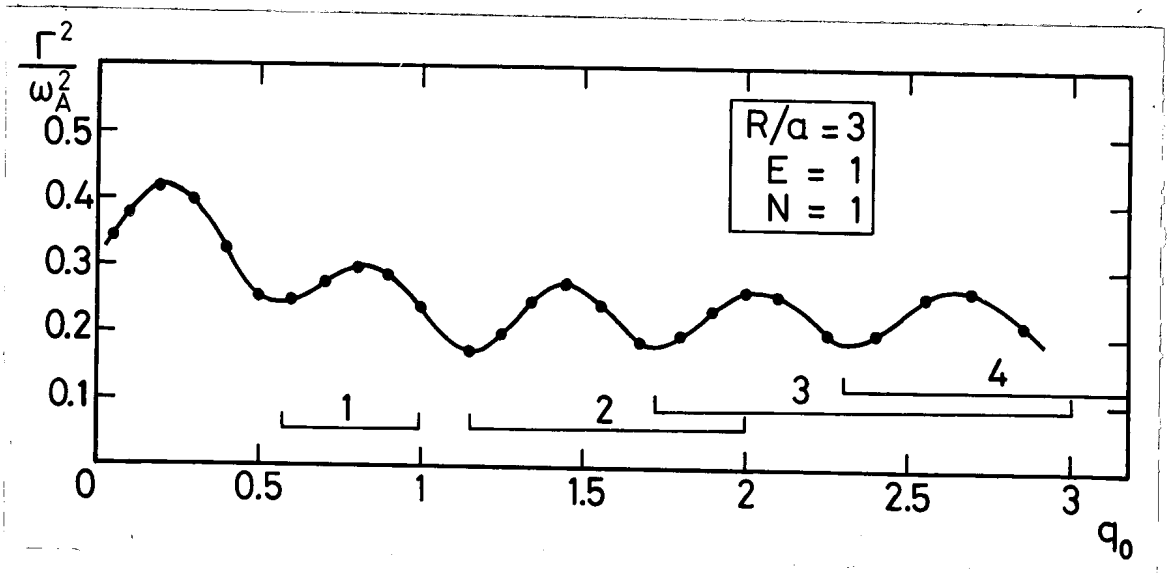
$\frac{\Gamma^2}{\omega_A^2}$
0.5
0.4
0.3
0.2
0.1
0
0.5
1
1.5
2
2.5
3
q_0
R/a = 3
E = 1
N = 1
1
2
3
4

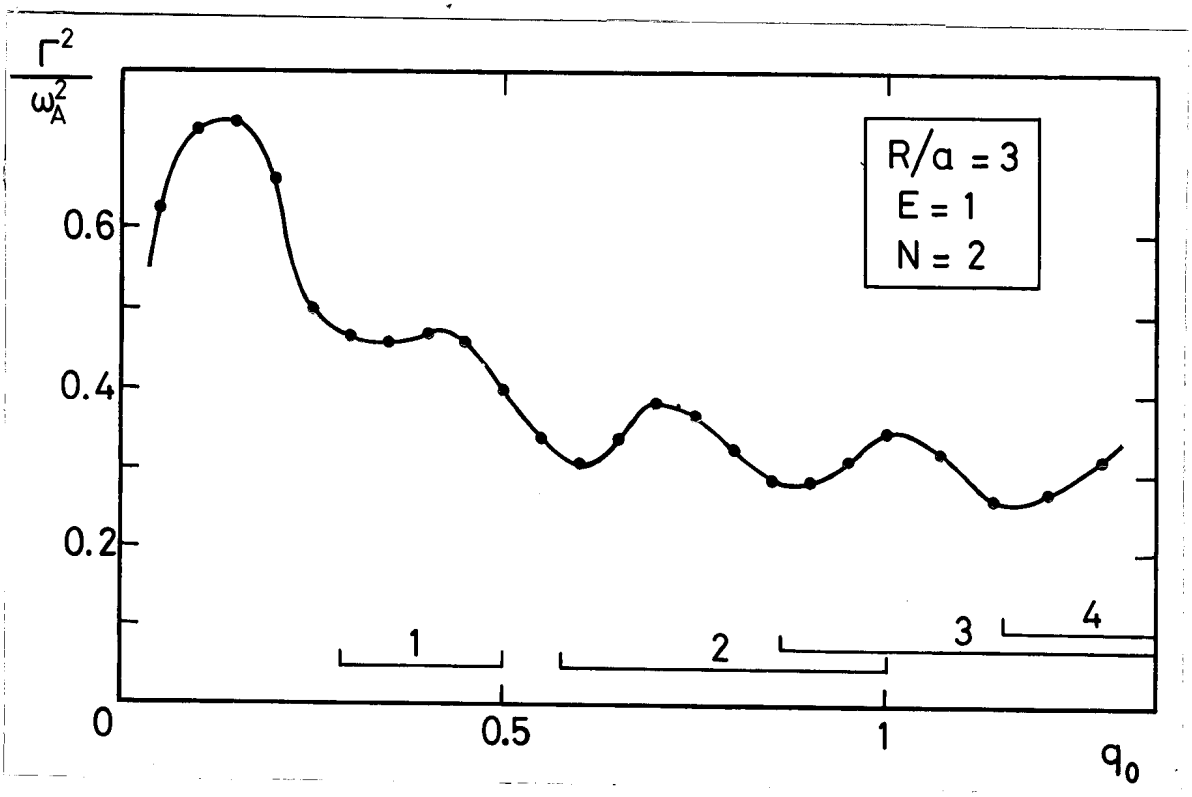
$\frac{\Gamma^2}{\omega_A^2}$
0.6
0.4
0.2
0
0.5
1
q_0
R/a = 3
E = 1
N = 2
1
2
3
4

FIGURE 3

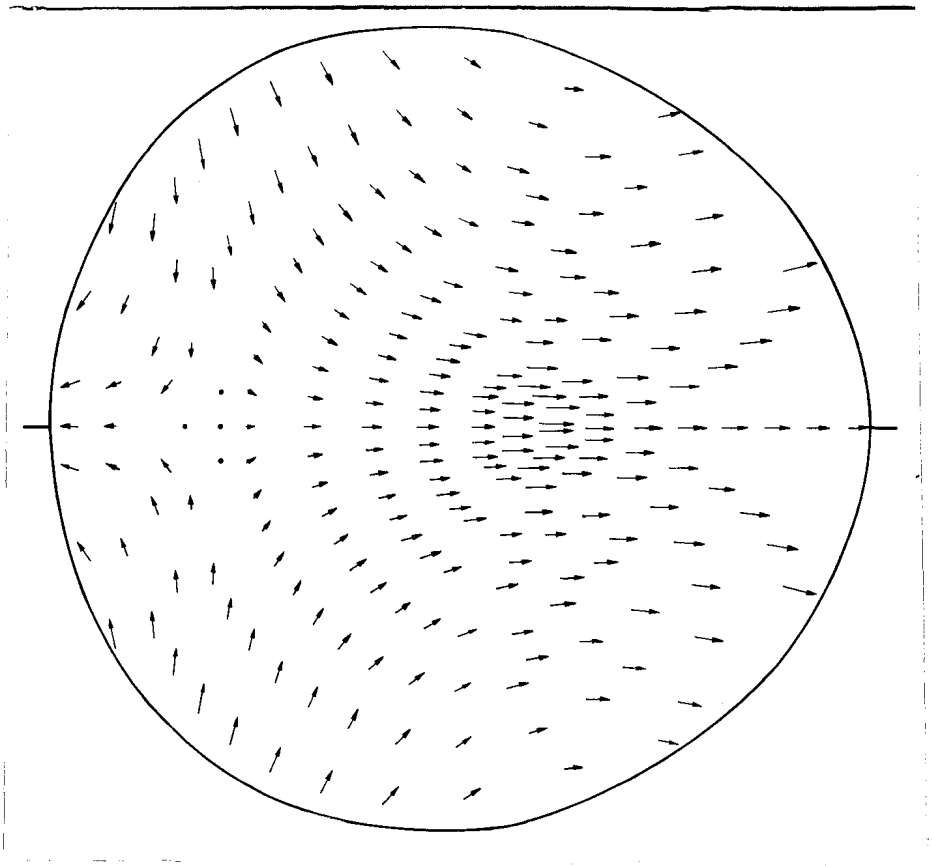

FIGURE 4

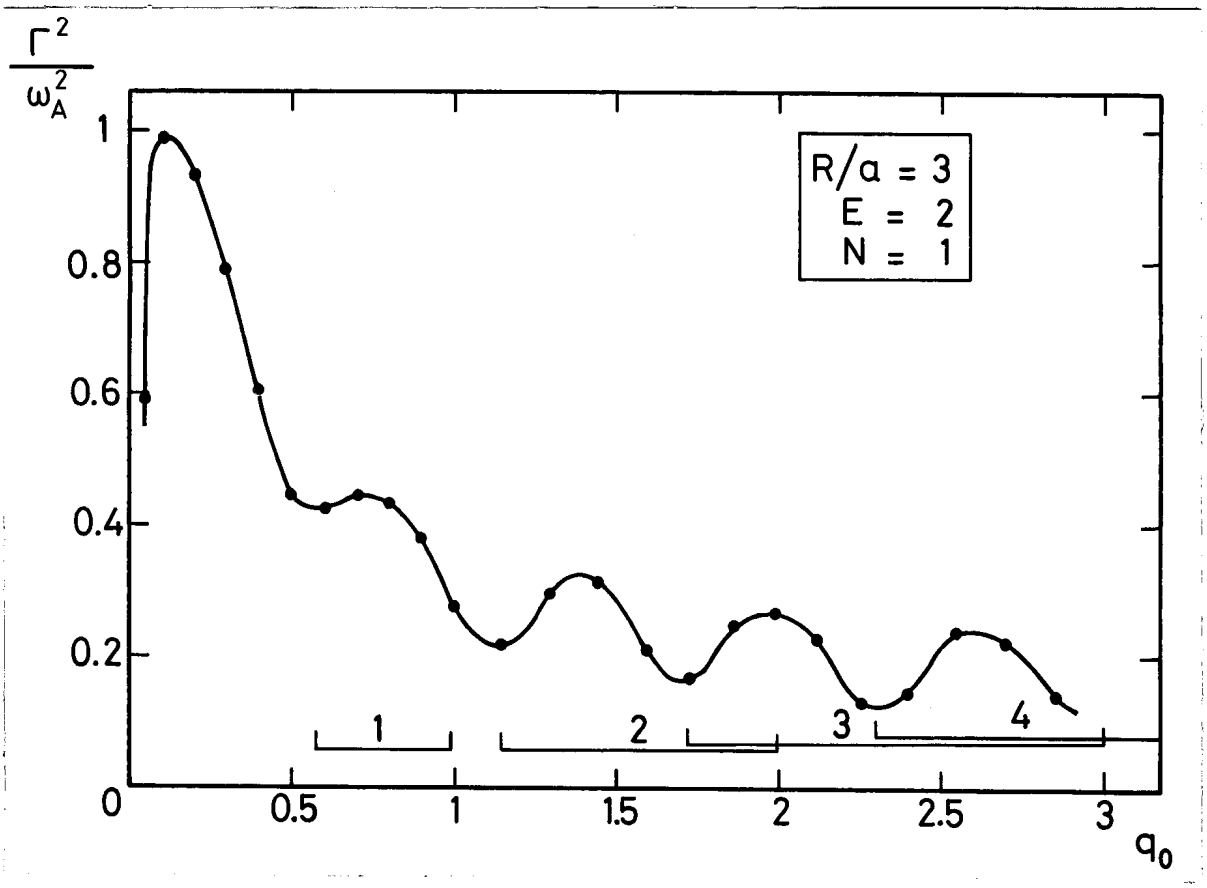

FIGURE 5

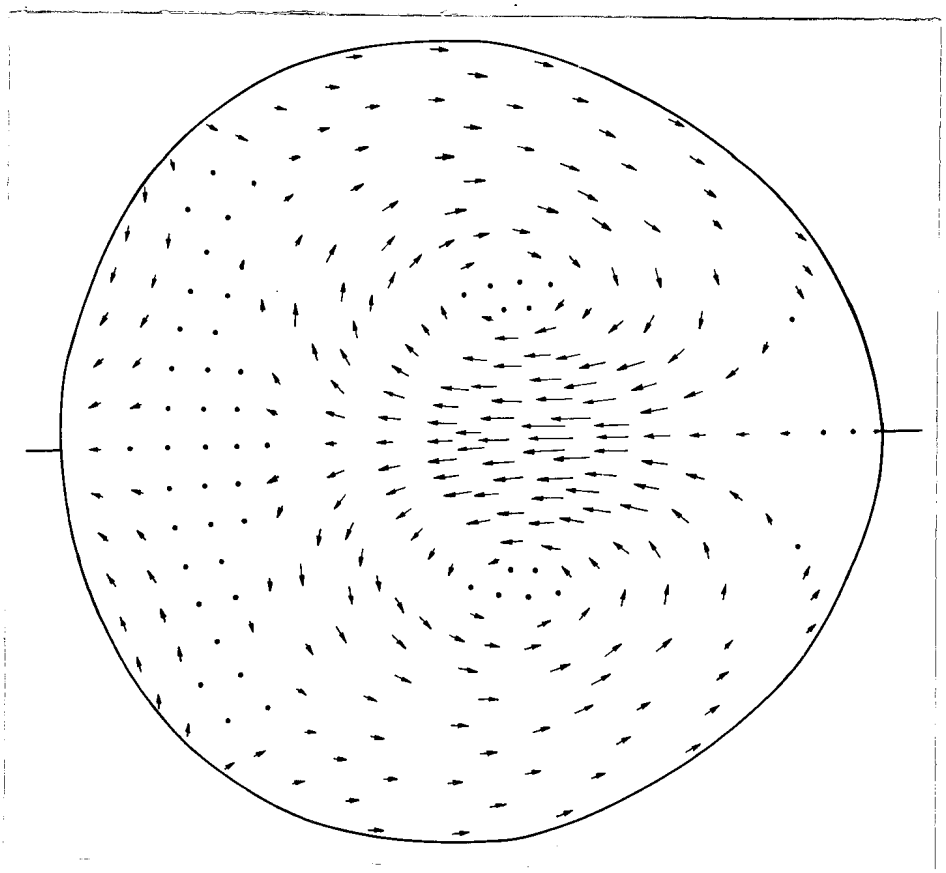

FIGURE 6